

Calibration of Solid State Nuclear Track Detectors for Rare Event Searches

M. Kalliokoski, G. Leví, A. Maulik^{*2,3}, I. Ostrovskiy, L. Patrizi, J. Pinfold[†], Z. Sahnoun[†], G. Sirri, R. Solu, M. Staelen, V. Toghiani, and A. Upreti

¹*Helsinki Institute of Physics, University of Helsinki, Helsinki, Finland*

²*INFN Section of Bologna and DIFA University of Bologna, Bologna, Italy*

³*Physics Department, University of Alberta, Edmonton, Alberta, Canada*

⁴*Department of Physics and Astronomy, University of Alabama, Tuscaloosa, USA*

⁵*IFIC, Universitat de Valencia-CSIC, Valencia, Spain*

Abstract

The calibration of the CR39 and Makrofol Nuclear Track Detectors of the MoEDAL experiment at the CERN-LHC was performed by exposing stacks of detector foils to heavy ion beams with energies ranging from 340 MeV/nucleon to 150 GeV/nucleon. After chemical etching, the base areas and lengths of etch-pit cones were measured using automatic and manual optical microscopes. The response of the detectors was measured by the ratio of the track-etching rate over the bulk-etching rate, which was determined over a range extending from their threshold at $Z/\beta \sim 7$ and ~ 50 for CR39 and Makrofol, respectively, up to $Z/\beta \sim 92$.

Keywords: Particle tracking detectors, Detector alignment and calibration methods (particle-beams), Particle identification methods.

1 Introduction

Solid State Nuclear Track Detectors (SSNTDs) are widely used in several scientific applications, such as nuclear fragmentation studies [1], cosmic ray composition and exotic particles searches in the cosmic radiation and at particle accelerators [2, 3, 4, 5, 6, 7]. They are often the detectors of choice when it comes to the search for highly ionizing particles in a background dominated by minimum ionizing particles.

^{*}Corresponding author at anu.maulik@bo.infn.it

[†]Corresponding author at sahnoun@bo.infn.it

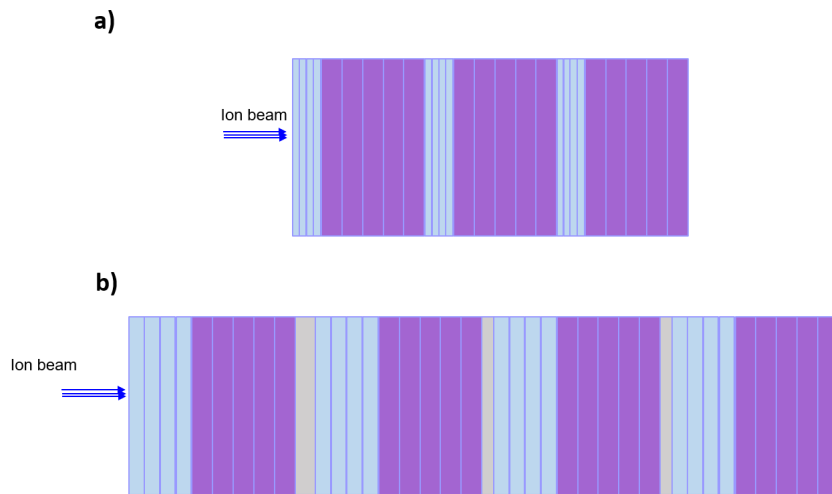


Figure 1: Scheme of calibration stacks; a) stack composed of several CR39 foils; b) stacks with one or two 9.5 mm thick aluminum slabs interleaved to groups of SSNTDs foils. In blue are CR39 foils 0.5 or 1 mm thick, in purple are CR39 foils 1.5 mm thick and in grey are the aluminum slabs.

A charged particle crossing a foil of plastic SSNTD breaks the polymeric bonds in a narrow ($O(10\text{ nm})$) cylindrical region (“latent track”) along its trajectory. By a suitable chemical etching process, which acts preferentially along the latent track, conical “etch-pits” are formed. Ionizing particles will exhibit a distinct signature characterized by continuous tracks with significant and consistent dimensions through multiple layers of SSNTDs.

Calibrations of CR39 and Makrofol have been performed in the past [8, 9]. Since the response of SSNTDs depends very sensitively on applied etching conditions a re-calibration becomes necessary whenever the detectors are deployed for a new experiment.

In this paper we report the results of the calibration of the CR39 manufactured by TASL Ltd, and, Makrofol produced by Bayer Films LLC, which are both used in the SSNTD sub-detector of the MoEDAL experiment at the Large Hadron Collider (LHC) located at the European Centre for Nuclear Research (CERN). MoEDAL is designed to search for Highly Ionizing Particle (HIPs) such as magnetic monopoles and highly electrically charged particles [10, 11]. In MoEDAL stacks of CR39 and Makrofoils are deployed over a surface about 10 m^2 around the Interaction Point (IP8) shared with the LHCb experiment.

Table 1: Ions used for the calibration of CR39 at NSRL. Z/β and REL are the charge to velocity ratio, and the restricted energy loss of the beam ions, respectively.

Ions	Kinetic energy (MeV/nucleon)	Z/β	REL (MeVg ⁻¹ cm ²)
¹² C ⁶⁺	1000	6.9	42.6
¹⁶ O ⁸⁺	1000	9.2	75.8
²⁸ Si ¹⁴⁺	1000	16.2	232.2
²⁸ Si ¹⁴⁺	715	17.2	256.3
²⁸ Si ¹⁴⁺	555	18.3	281.9
²⁸ Si ¹⁴⁺	450	19.3	309.2
⁵⁶ Fe ²⁶⁺	1000	30.0	800.8
⁵⁶ Fe ²⁶⁺	340	39.1	1232.2
⁸⁴ Kr ³⁶⁺	383	52.1	2215.6
¹²⁹ Xe ⁵⁴⁺	350	80.4	5209.4

2 Experimental Method

The calibration process adopted for the MoEDAL SSNTDs involves the exposure of the detectors to heavy ion beams at particle accelerators. etched foils undergo chemical etching in aqueous solutions of KOH or NaOH, at concentrations typically of 4N - 6N, and temperatures of 50, resulting in the formation of conical etch pits. The shape and size of etch pits depend on the particle's restricted energy loss (REL), its angle of incidence and the etching condition.

2.1 Exposure and Etching of CR39

Stacks of SSNTD layers composed of 11.5 cm × 11.5 cm of foils, 0 and 1.5 mm thick, were exposed in 2021 at the NASA Space Radiation Laboratory (NSRL) to ¹²C⁶⁺, ¹⁶O⁸⁺, ²⁸Si¹⁴⁺, ⁵⁶Fe²⁶⁺, ⁸⁴Kr³⁶⁺, and ¹²⁹Xe⁵⁴⁺ ion beams with energies ranging from 340 MeV/nucleon to 1 GeV/nucleon. initial values of ions' kinetic energy, charge on β ratio (Z/β) and restricted energy loss (REL) are listed in Table 1. Exposures were performed with ions impinging normally on the detector surface.

The exposed stacks comprised layers of CR39 and other SSNTDs such as Makrofoland PET (Figure 1a). In order to slow down incident ions, slabs of aluminium, 9.5 mm and 19 mm thick (Figure 1b) were introduced in some stacks. Passing through the plastic foils and the aluminium slabs, ion's kinetic energy and charge Z decrease, while the value of REL and ratio Z/β increase. Since along their path ions can undergo charge-changing fragmentation, with a single exposure it is possible to probe the response of

CR39 to a wide range of nuclear charge and energy losses.

Figure 2a shows the variation of $^{84}\text{Kr}^{36+}$ ions' kinetic energy along a stack of CR39 foils. Figure 2b shows, for the same ions, the Z/β versus depth in the stack. Figures 3a,b show the kinetic energy and Z/β , respectively, of $^{56}\text{Fe}^{26+}$ ions along a stack composed of CR39 foils and aluminum slabs.

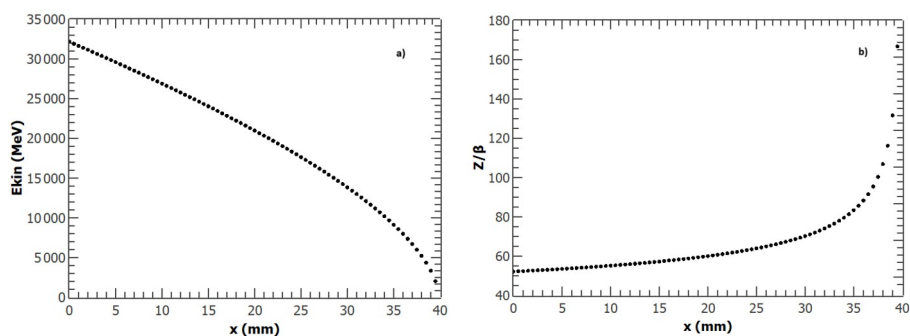


Figure 2: Kinetic energy (a) and (b) Z/β ratio of Kr ion across a 40 mm thick CR39 foils

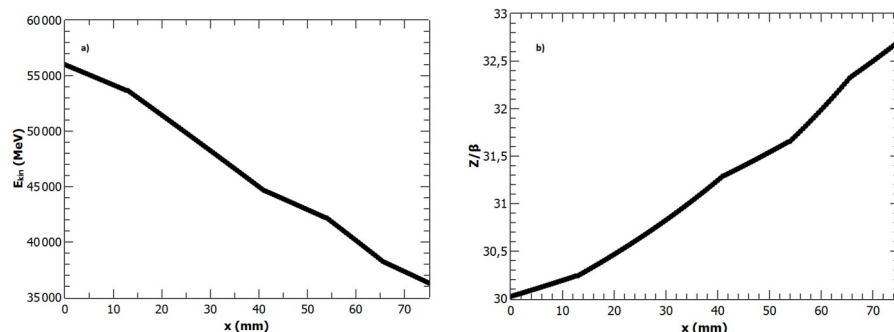


Figure 3: Kinetic energy (a) and (b) Z/β of Fe ion across 70 mm thick stack composed of CR39 foils and aluminum slabs. The change in slope corresponds to transitions from a group of CR39 foils to an Aluminum slab.

After exposure the CR39 foils were etched in 6N NaOH solution at $(70.0 \pm 0.1)^\circ\text{C}$ for 15 h. For ions impinging normally to the surface, in the present case, surface openings of etch-pits observed under an optical microscope manifest as dark circles, referred to also as "tracks". Figure 4 shows tracks of ^{16}O , ^{28}Si , ^{56}Fe and ^{84}Kr ions in CR39.

The CR39 bulk etching rate, v , was determined for each detector foil, by measuring its thickness before and after etching with an accuracy of

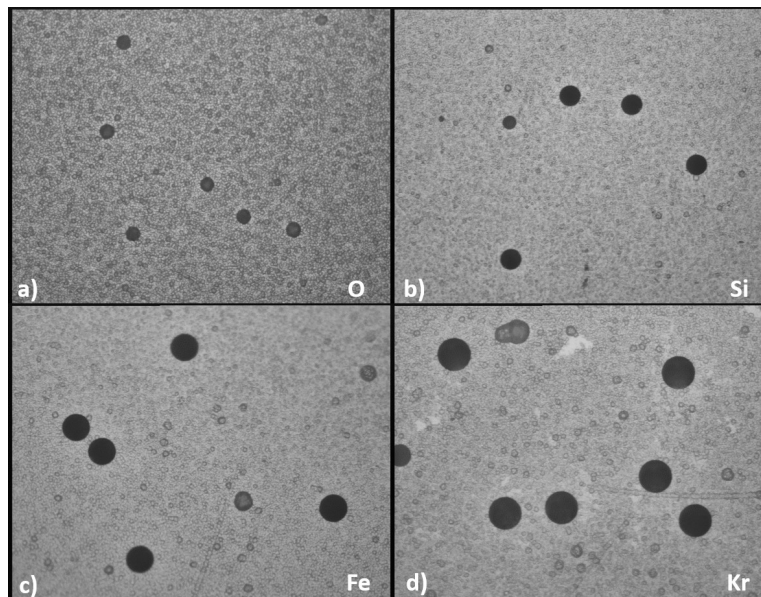


Figure 4: Ion tracks in CR39 after 15 hours etching in 6 N NaOH solution at 70°C as seen under an optical microscope with 20× objective coupled to a CCD camera from top left clockwise: Oxygen ions, $Z/\beta = 9$; Silicon ions, $Z/\beta = 24$; Krypton ions, $Z/\beta = 52$ and Iron ions, $Z/\beta = 39$.

$1\mu\text{m}$ on a grid of 20 points. The average v_B is $(1.27 \pm 0.05) \mu\text{m/h}$. The v_B of the foils ranges from $(1.1 \pm 0.05) \mu\text{m/h}$ up to $(1.5 \pm 0.05) \mu\text{m/h}$.

2.2 Exposure and Etching of Makrofol

The process is very similar to the one applied to the CR39. The main difference concerns the etchant. It has been observed that for Makrofol, the inclusion of Ethyl Alcohol in the etching solution has a polishing effect on the Makrofol surface which results in a smoother surface and sharper etch-pit edges. Commercial Ethyl Alcohol contains 1 % of additives such as methyl ethyl ketone (MEK), isopropyl alcohol (IPA), and denatonium benzoate introduced during the denaturing process. The types and amount of additives in Ethyl Alcohol were changed according to EU regulations issued in 2013 and in 2017. Experimental investigations revealed that Ethyl Alcohol prepared according to the 2013 EU regulations yielded the most favorable etching results. Since then, Makrofol detectors were etched using this specific type of Ethyl Alcohol. An agreement has been established with the manufacturer to ensure a consistent supply of this particular variety.

Several stacks of Makrofol foils measuring $11.5 \text{ cm} \times 11.5 \text{ cm}$ and with a thickness of $500 \mu\text{m}$ were exposed to $156 \text{ GeV/nucleon } ^{82}\text{Pb}$ and $13 \text{ GeV/nucleon } ^{54}\text{Xe}$ nuclei at the CERN-SPS in 2017 and 2018. Upstream

foils in the stacks served both as a detector and fragmentation target; downstream foils recorded both Pb and Xe ions along with their fragments.

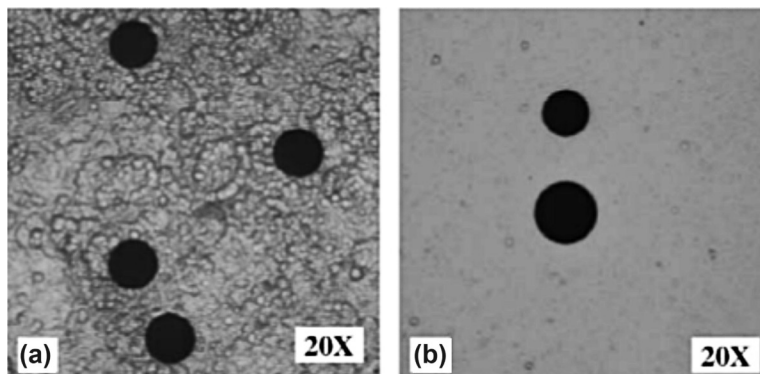


Figure 5: Tracks of Pb and Xe ions, and their nuclear fragments in Makrofol after 15 h etching in 5.5N KOH + 20 % Ethyl Alcohol solution at 45

After exposure Makrofol foils were etched in 5.5N KOH + 20 % Ethyl Alcohol at $(45.0 \pm 0.1)^\circ\text{C}$ for 15 h. The bulk etching rate determined by measuring the mean thickness of the foils before and after etching was $v = (3.01 \pm 0.05) \mu\text{m/h}$. The application of the selected etching condition resulted in well-defined conical etch-pits with sharp edges against a clear surface as shown in figure 5.

3 Etch-pit measurements

After etching, the base areas of conical etch-pits in CR39 and Makrofol foils were measured using an automated microscope featuring a stage with automated movements in the X and Y directions and automatic focusing on each frame. It was coupled to a computer equipped with image analysis software. The distributions of track areas in CR39 foils for different ion species are shown in figure 6.

Figure 7 illustrates the area distribution of lead ion tracks and their fragments in Makrofol. The distributions in figure 6 and in figure 7 are obtained by averaging the measurements of etch-pit surface areas on both the front and back surfaces of two or three successive foils in a stack after correctly aligning the reference frames of all surfaces to a unique one. This procedure enhances charge resolution.

Both in CR39 and in Makrofol the charge resolution decreases for $Z/\beta \geq 75$. For larger Z/β values, charge resolution can be recovered by measuring the etch-cone length. For the calibration of Makrofol, etch-pits with the largest surface areas were selected and their lengths were manually measured using a Leica DMRME microscope with a resolution of $1 \mu\text{m}$. Figure 8 and

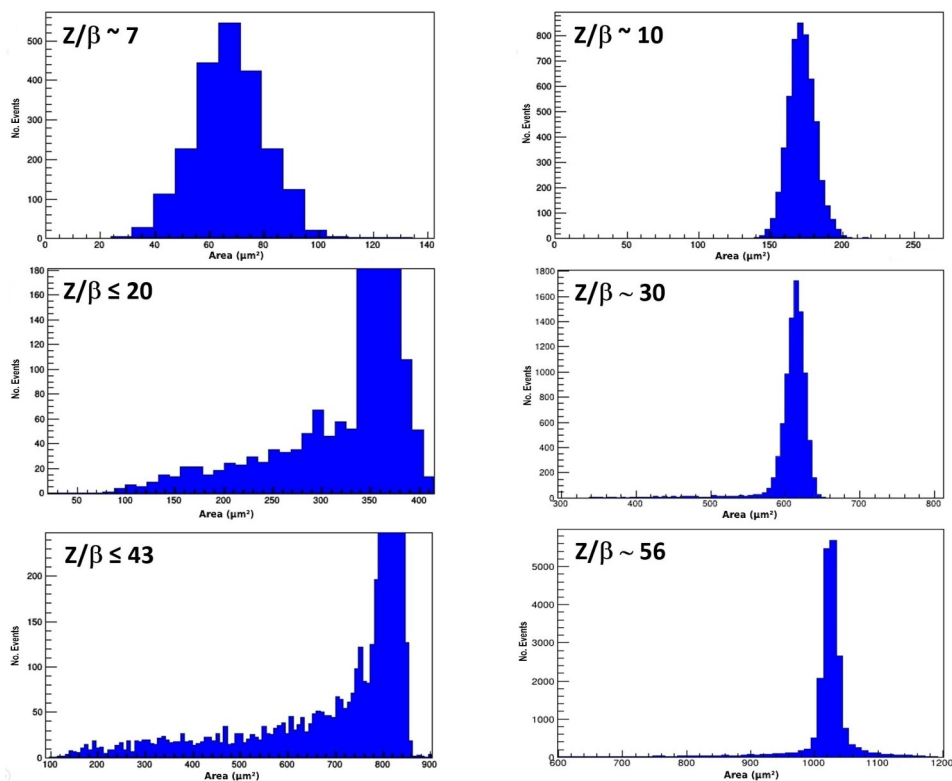


Figure 6: Distributions of etch-pits base area measured in CR39 foils, exposed to Carbon ions (upper left), Oxygen ions (upper right), Silicon ions (center left), Iron ions (center right and lower left) and Krypton ions (lower right). Distributions are obtained from foils exposed to different ions, for different positions in the stacks, first layers for Carbon, Oxygen and Iron (center right) ions and innermost layers for Silicon, (lower left) and Krypton ions.

figure 9 show the distributions of etch-pit lengths in CR39 and in Makrofol, respectively.

4 The reduced etch-ratio versus REL

The ratio $\rho = v_T/v_B$, where v is the etching rate along the latent track, is used to evaluate the detector response (referred to as “etch-rate” in the following). The etch-rate was determined using eq. (1) if the surface track area A was available and eq. (2) if the etch-pit length L_e had been measured [8]. In both equations t is the etching duration and L_e is the cone length obtained by taking into account the CR39 or Makrofol refractive index (~ 1.498 and ~ 1.58 , respectively).

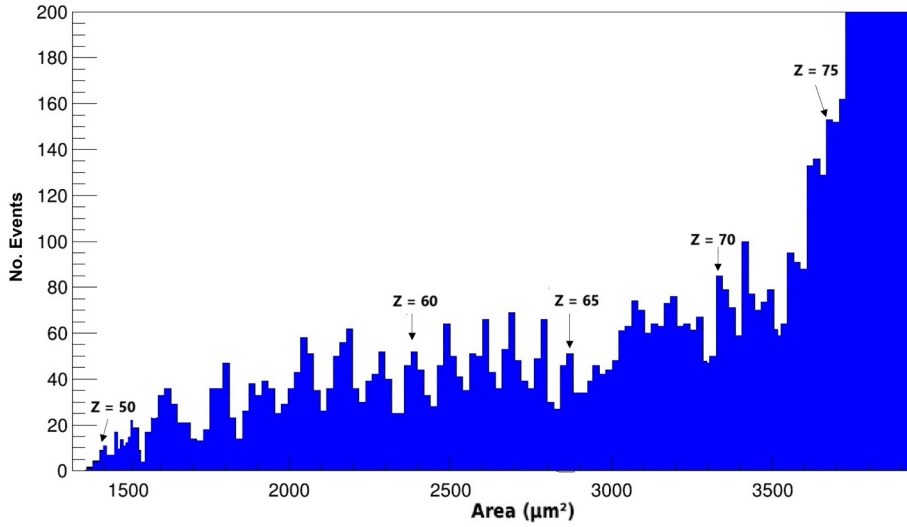


Figure 7: Etch-pit base area distribution of lead ions and charged nuclear fragments in Makrofol.

$$\rho = \frac{1 + \frac{A/\pi}{(v_B t)^2}}{1 - \frac{A/\pi}{(v_B t)^2}} \quad (1)$$

$$\rho = 1 + \frac{L_e}{v_B t} \quad (2)$$

A Monte Carlo simulation of the ions' propagation through the stacks was implemented. The energy loss was computed using the SRIM [12] package. The ion's energy was evaluated after every detector layer or aluminum absorber with $\sim 10\%$ accuracy. The reduced etch rate $\rho - 1$ versus REL for CR39 is plotted in figure 10. The detector's threshold, defined as the value of REL corresponding to $\rho = 1$, is at $\sim 40 \text{ MeV cm}^{-2}$, which corresponds to the restricted energy loss of relativistic $Z/\beta = 7$ Nitrogen ion. Calibration data extend up to an equivalent relativistic charge $Z/\beta \sim 92$. The dashed curve in figure 10 is a 4-degree polynomial fit:

$$\rho - 1 = a_0 + a_1 \times REL + a_2 \times REL^2 + a_3 \times REL^3 + a_4 \times REL^4, \quad (3)$$

with parameters $a_0 = 0.0297 \pm 0.059$, $a_1 = (3.08 \pm 0.44) \times 10^3$, $a_2 = (-1.47 \pm 0.52) \times 10^6$, $a_3 = (5.96 \pm 1.77) \times 10^9$ and $a_4 = (-3.84 \pm 1.71) \times 10^{14}$, and $\chi^2/dof = 1.28$.

The reduced etch-rate $\rho - 1$ versus REL for the Makrofol NTD is shown in figure 11. The detection threshold is at $\sim 2700 \text{ MeV cm}^{-2}$, corresponding to a relativistic nuclear fragment with charge $Z/\beta \sim 50$. The dashed curve is a 4-degree polynomial fit, as in eq. 3, with parameters:

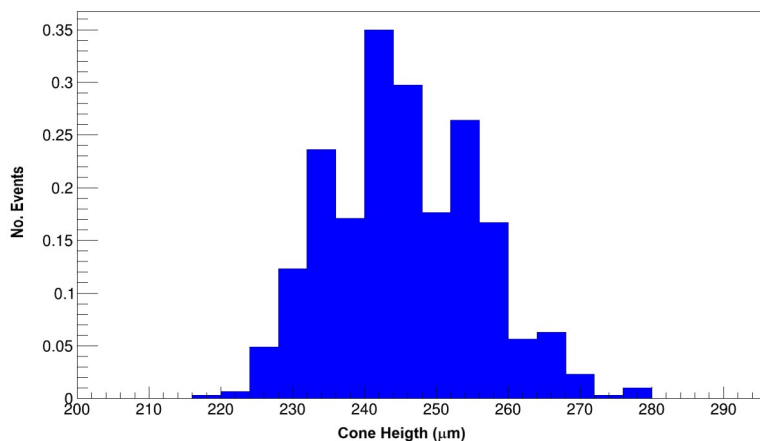


Figure 8: Normalized distribution of track-pit lengths of ^{129}Xe ions and their fragments in CR39. The distribution is obtained by combining data from two successive foils with different measurement statistics, resulting in a total of slightly less than 500 measurements.

$$(-1.37 \pm 1.03) \times 10^0, a_1 = (-1.42 \pm 1.00) \times 10^0, a_2 = (9.61 \pm 3.52) \times 10^0$$

$$a_3 = (-1.76 \pm 0.53) \times 10^{10} \text{ and } a_4 = (1.24 \pm 0.29) \times 10^{14}, \text{ and } \chi^2/dof = 0.3.$$

5 Conclusions

The response of CR39 and Makrofol solid state nuclear track detectors used in the MoEDAL experiment was calibrated using several ions at different energies covering a large Z/β range. The CR39 can detect particles with a restricted energy loss as low as $40 \text{ MeV}^2/\text{g cm}^2$ or equivalently with $Z/\beta = 7$, up to $\text{REL} \sim 7000 \text{ MeV}^{-1} \text{g cm}^2$, or equivalently $Z/\beta = 92$. Makrofol on the other hand is shown to have a higher detection threshold and can only detect particles with a restricted energy loss of at least $2700 \text{ MeV}^2/\text{g cm}^2$ or equivalently $Z/\beta = 50$.

In conclusion, both CR39 and Makrofol are shown to be excellent choices as detectors for a wide range of applications where the detection of heavy ions against a low-Z background is important such as in Nuclear Physics fragmentation, Cosmic Ray composition etc. They are also important in the search for heavily ionizing rare events, which a clear signature is expected over all possible backgrounds. CR39 and Makrofol have already made a significant contribution to setting limits on the production of predicted charged exotic particles and can potentially contribute to a discovery.

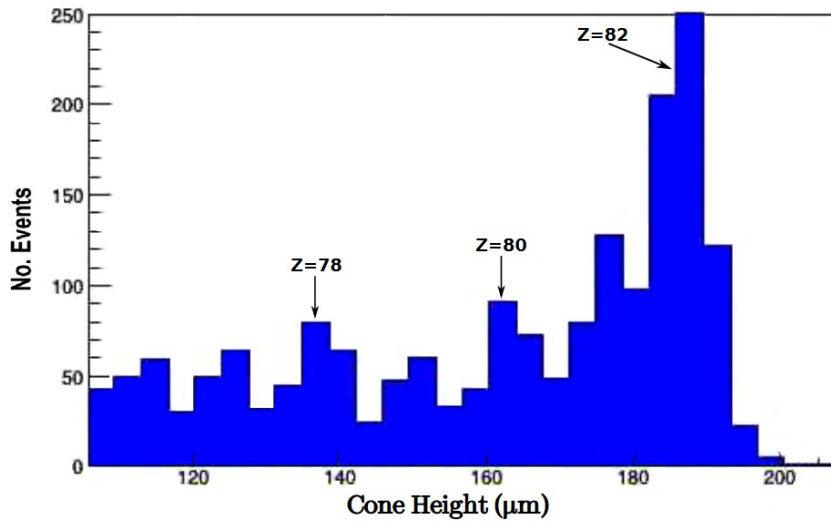


Figure 9: The etch-cone length distribution for Pb and its fragments on Makrofol, showing well defined peaks for large ion charges.

Acknowledgments

The authors sincerely thank the staff at CERN-SPS and NSRL for their help during the irradiation of the SSNTD stacks. The work of A. Maulik was supported by the University of Alberta, Canada and that of AUpreti by the NSF grant 2309505 of the MoEDAL group at the University of Alabama, USA.

References

- [1] S. Cecchini et al., *Fragmentation cross sections of $^{26}\text{FeSi}^{14+}$ and C^{6+} ions of 0.3-10 A GeV on polyethylene, CR39 and aluminum targets*, *Nucl. Phys. A* **807** (2008) 206, arXiv:0801.3195.
- [2] T. Chiarusi et al., *First results of the CAKE experiment*, *Radiat. Meas.* **36** (2003) 335.
- [3] E. Medinaceli et. al, *Magnetic monopole search at high altitude with the SLIM experiment*, *Radiat. Meas.* **44** (2009) 889.
- [4] R. Bhattacharyya et al., *Study of radiation background at various high altitude locations in preparation for rare event search in cosmic rays*, *JCAP* **04** (2017) 035.

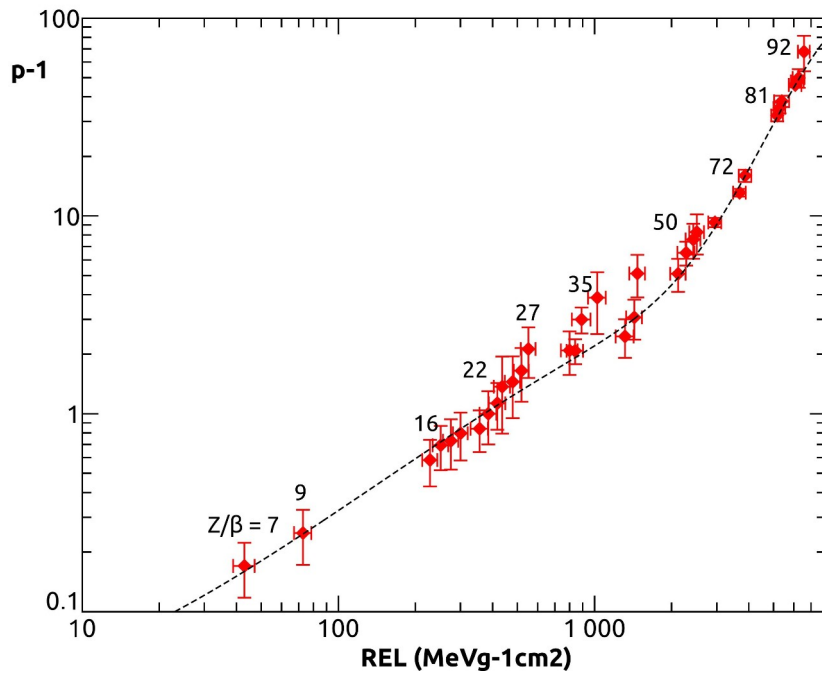


Figure 10: Reduced etch-rate of CR39 versus REL. The dashed curve is a 4-degree polynomial fit to the data (see text).

- [5] H. Hoffmann, G. Kantardjian, S.D. Liberto et al. *A new search for magnetic monopoles at the CERN-ISR with plastic detectors.* *Lett. Nuovo Cimento* **23** (1978) 357-360.
- [6] G. Giacomelli, A.M. Rossi, G. Vannini et al. *Search for magnetic monopoles at the CERN-ISR with plastic detectors.* *Nuovo Cimento* **A 28** (1975) 21-28.
- [7] E. Amaldi, G. Baroni and G. Romano *Proposal of an experiment for searching Dirac magnetic monopoles at the ISR with plastic technique.* CERN-ISRC-70-8 (1970).
- [8] G. Giacomelli et al. *Extended calibration of a CR39 nuclear track detector with 158 A GeV ^{207}Pb ions,* *Nucl. Instr. and Meth. A* **411** (1998) 41.
- [9] S. Balestra, et. al, *Bulk etch rate measurements and calibrations of plastic nuclear track detectors,* *Nucl. Instr. and Meth. B* **254** (2007) 254.

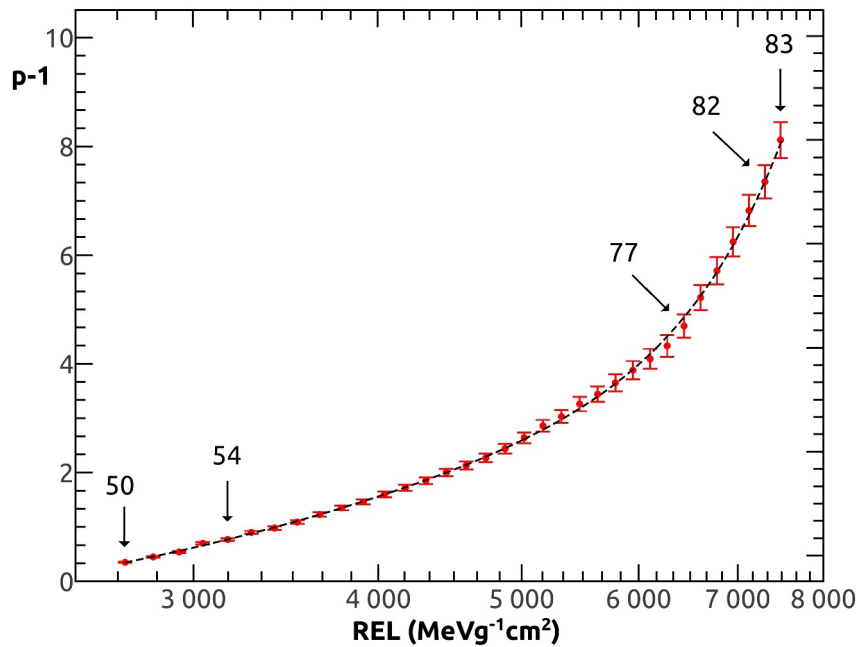


Figure 11: Reduced etch rate $p-1$ versus REL for Makrofol SSNTD exposed to relativistic lead and xenon ion beams. The dashed curve represents a polynomial fit.

- [10] MoEDAL Collaboration, B. Acharya et al., *The physics programme of the MoEDAL experiment at the LHC*, *Int. J. Mod. Phys. A* **29** (2014) 1430050, arXiv:1405.7662 [hep-ph].
- [11] J. Pinfold, *The MoEDAL experiment: a new light on the high-energy frontier*, *Phil. Trans. R. Soc. A* **377** (2019) 0382.
- [12] F. Ziegler, M.D. Ziegler, J.P. Biersack, *The Stopping and Range of Ions in Matter*, *Nucl. Instr. and Meth. B* **268** (2010) 1818.